Staropoli *et al. Chem. Biol. Technol. Agric.* (2023) 10:28
https://doi.org/10.1186/s40538-023-00383-x

Chemical and Biological Technologies in Agriculture

RESEARCH

Open Access

Induced secondary metabolites of the beneficial fungus *Trichoderma harzianum* M10 through OSMAC approach

Alessia Staropoli[1,2], Giuseppina Iacomino[1], Paola De Cicco[3], Sheridan L. Woo[3,5], Luigi Di Costanzo[1] and Francesco Vinale[2,4,5*]

Abstract

Background Fungi biosynthesize a wide range of chemically diverse secondary metabolites during processes of competition with other micro- and macro-organisms, symbiosis, parasitism, or pathogenesis. Some of these natural compounds have antibiotic properties, which allow the microbe to inhibit and/or kill their microbial competitors.

Results In the course of an ongoing search for novel bioactive metabolites from *Trichoderma harzianum* M10 using OSMAC (One Strain MAny Compounds) strategy, a bioactive chromone derivative has been isolated. The 5-hydroxy-2,3-dimethyl-7-methoxychromone (**1**), purified for the first time from *T. harzianum* M10 and induced in specific medium (potato dextrose broth, PDB) and condition (light and shaking), has been obtained as pure crystals and its structure has been fully characterized using X-ray and spectroscopic methods. This metabolite revealed a significant antibiotic activity against *Rhizoctonia solani* (45% of growth inhibition after 24 h of incubation at a concentration of 100 ng plug^{-1}) and significantly reduced the viability of colorectal human cancer cells in a concentration-dependent manner. Moreover, metabolomic analysis allowed the identification of compounds modulated by the cultivating conditions. Among the statistically different molecules detected it was possible to identify siderophores, such as ferricrocin and coprogen B, harzianic acid (and its derivatives), and butenolides.

Conclusion OSMAC strategy represents a valuable approach to overcome the limitations of experiments performed under laboratory conditions. Indeed, it is possible to modulate metabolites production by changing medium and conditions applied to the cultures. A specific set of conditions induced the production of a secondary metabolite never isolated from *T. harzianum* M10. The compound, a methoxychromone derivative, characterized by X-ray diffraction, mass spectrometry, IR, and NMR, displayed antimicrobial and antitumor activities.

Keywords *Trichoderma*, 5-Hydroxy-2,3-dimethyl-7-methoxychromone, Ferricrocin, Coprogen B, Harzianic acid, Butenolides, OSMAC strategy, Biocontrol, Metabolomic

*Correspondence:
Francesco Vinale
frvinale@unina.it
Full list of author information is available at the end of the article

Graphical Abstract

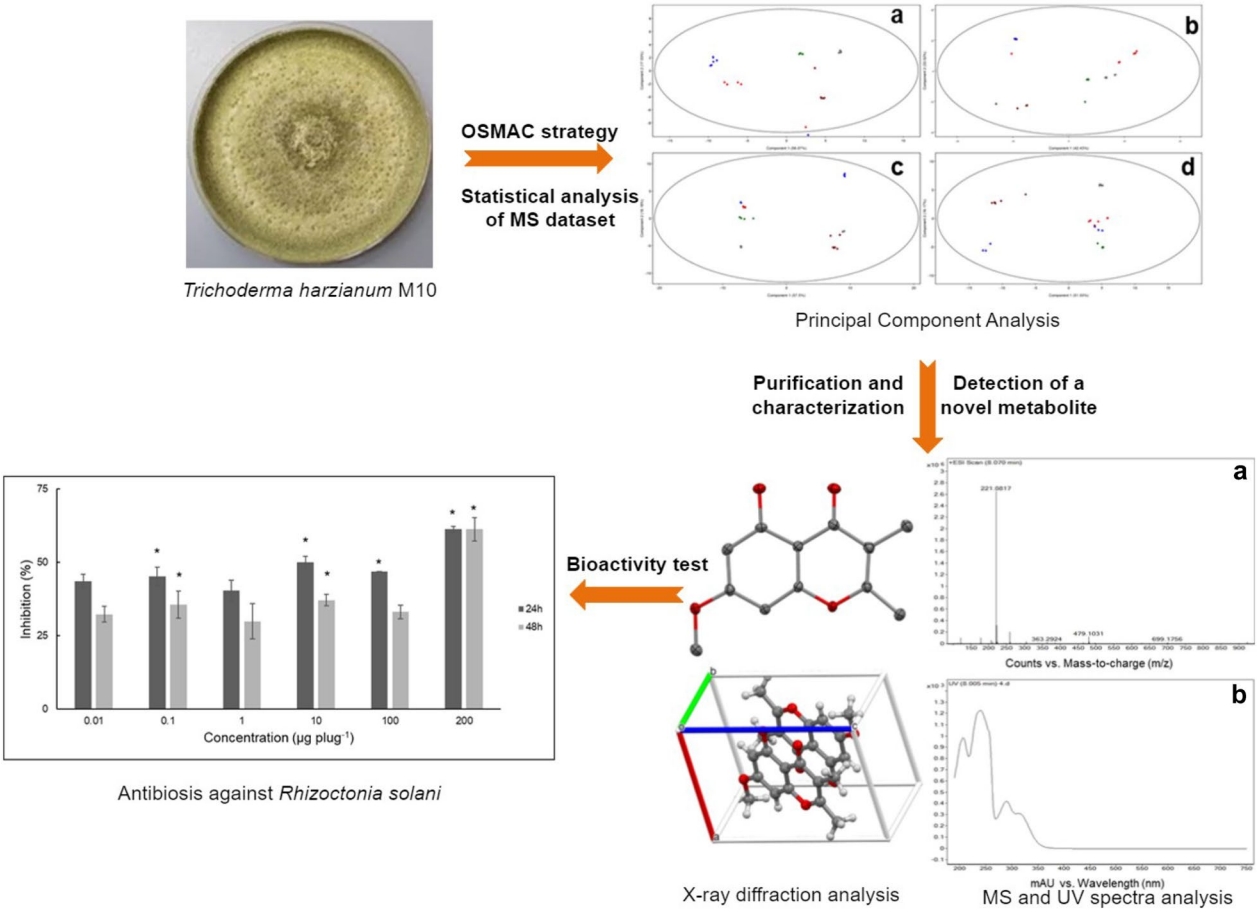

Introduction

Fungi of the genus *Trichoderma* are successfully used in agriculture due to their aptitude to act as biocontrol agents and to stimulate plant growth and resistance to biotic and abiotic stress [1]. Numerous studies have been conducted to characterize the factors involved in the interactions of *Trichoderma* sp. with the plant and the pathogen with the aim to discover specific molecules with a direct and/or indirect activity [2, 3]. Recently, metabolomics has been extensively applied to select beneficial strains and their "effectors" or to identify factors established by these beneficial microorganisms with their microenvironment [4–8].

Several strains of *Trichoderma* are well-known producers of bioactive secondary metabolites [9, 10]. *Trichoderma* produces natural compounds involved in the beneficial interactions with the plants [11, 12]. Microbes can synthetize a wide range of metabolites, but purification of known compounds is frequent since some biosynthetic genes are not transcribed in vitro or under standard laboratory conditions. Many genes are silent and such clusters can be activated using specific elicitors and/or in specific conditions [13]. OSMAC (One Strain MAny Compounds) strategy is based on the application of a variety of growing environments on a selected fungal (or other microbial) strain to induce biosynthesis of secondary metabolites [14]. This approach can be applied using different methods, such as (1) varying the composition of the media, salinity, and pH; (2) using solid or liquid medium, and by adding solvents (i.e.,

DMSO, methanol, etc.) or trace elements (i.e., halogens; metal cations or rare earth cations); and (3) modifying growth temperature, light or darkness, oxygen concentration, vessel type, and static or shaking conditions [15]. To overcome the laboratory limitations, it is also possible to cultivate fungi by simulating naturally occurring conditions, where microbes co-exist within complex communities, generally referred as the "microbiome" [15]. This method can be used to elicit the production of novel bioactive compounds through the co-cultivation of selected microbial strains in a specific growing environment [16–18].

In the course of an ongoing search for secondary metabolites from *T. harzianum* M10, a bioactive methoxychromone derivative (**1**) was identified by using OSMAC strategy to up-regulate the genes involved in the biosynthesis of this compound. After growing M10 strain in an inductive liquid medium, the cultural filtrate was exhaustively extracted with ethyl acetate and the crude extract was fractionated by direct phase column chromatography. A compound, obtained as pure crystal from one of the fractions, was identified as 5-hydroxy-2,3-dimethyl-7-methoxychromone by X-ray analysis and spectroscopic studies. The compound, isolated for first time from a *T. harzianum* M10 culture, was tested at different concentrations for antifungal activity against the phytopathogenic agent *Rhizoctonia solani* and on colorectal human cancer cells.

Materials and methods

General experimental procedures

Fractionation with column chromatography was made on silica gel (Merck silica gel 60 GF_{254}), and TLC (thin-layer chromatography) silica gel GF_{254} plates (Merck Kieselgel 60 GF_{254}, 0.25 mm). The metabolites were detected on TLC plates with an UV lamp working at 254 or at 366 nm and/or by spraying with 5% (v/v) H_2SO_4 solution in EtOH (ethanol) followed by heating at 100 °C for 3 min. IR spectrum was recorded on a JASCO 4700 interferometer (JASCO International CO., LTD, Tokyo, Japan). Before being pressed and used as a solid support, the KBr powder was dried overnight at 120 °C.^{1}H NMR spectrum was recorded on a Bruker AMX instrument (AscendTM400, Bremen, Germany) at 400 MHz in $CDCl_3$. The same solvent was used as internal standard.

Microbial strains

T. harzianum strain M10 and *R. solani* were taken from the collection at University of Naples Federico II and maintained on Potato Dextrose Agar (HI-MEDIA, Pvt. Ltd., Mumbai, India) at 25 °C.

Growing conditions—OSMAC strategy

M10 was cultured in different liquid media and under different conditions to evaluate the modulation of metabolic profile. One 5 mm Ø plug was taken from the border of actively growing mycelium and inoculated into a 250-mL flask containing 100 mL of sterile medium. The media used for this experiment were Potato Dextrose Broth (PDB), 1/10 PDB, Yeast Peptone Glucose (YPD, 1% yeast extract, 2% peptone, 2% D-glucose) broth, Minimal Medium (MM, 3% sucrose, 0.05% KCl, 0.2% $NaNO_3$, 0.1% KH_2PO_4, 0.05% $MgSO_4 \times 7H_2O$) broth, and MM + 1 mM of iron chloride ($FeCl_3$). Each medium was incubated under white light or dark conditions and under rotation (140 rpm) or under static conditions for 15 days at 25 °C. Culture filtrates were obtained by pouring the liquid through Miracloth filter paper (Merck KGaA, Darmstadt, Germany) at atmospheric pressure. The experiment was carried out in triplicate.

Metabolites production in inducing liquid medium

Twelve 10 mm Ø plugs of M10, obtained from sporulated PDA cultures, were inoculated into 5 L flask containing 2.5 L of sterile PDB (HI-MEDIA, Pvt. Ltd., Mumbai, India). Four shaking liquid cultures were incubated at 25 °C and under white light for 21 days and then filtered through Miracloth filter paper at atmospheric pressure.

Metabolites extraction

Culture filtrate (10 L) was extensively extracted with ethyl acetate (EtOAc, Carlo Erba, Cornaredo, Milan, Italy) three times and the combined organic fractions were dried with sodium sulfate anhydrous (Na_2SO_4, Carlo Erba) and evaporated under vacuum at 40 °C in a rotary evaporator (RV 10, IKA®-Werke GmbH & Co. KG, Staufen, Germany). The crude extract thus obtained was resuspended in dichloromethane (DCM, Carlo Erba) at a concentration of 10 mg/mL and washed three times with sodium hydroxide (NaOH, Carlo Erba), to remove harzianic acid (HA), its stereoisomers, and derivatives [19].

The DCM residue, containing the methoxychromone derivative (**1**), was further purified by direct phase column chromatography (100 g of silica). Elution gradient was composed of petroleum ether (A, Carlo Erba) and EtOAc (B) as follows: 100% A, 80% A, 50% A, 20%A, and 100% B. Among the sixteen fractions collected, five contained compound **1**.

Liquid chromatography and gas chromatography–mass spectrometry analysis

Mass spectrometry coupled to liquid and gas chromatography techniques were exploited to characterize and

analyze culture filtrates of OSMAC strategy, the crude extract (EtOAc), and the chromatographic fractions.

LC–MS analysis

Analyses were conducted on a HP 1260 Infinity Series liquid chromatograph (Agilent Technologies, Santa Clara, CA, USA), equipped with a diode array detector (DAD, Agilent Technologies) and coupled to a high-resolution mass spectrometer (qTOF, Agilent Technologies). The reverse phase column used was an Adamas C18-X-Bond column (50 mm × 4.6 mm, 3.5 µm, Sepachrom Srl), the injection volume was 7 µL, and the system operated in positive ionization mode. Elution gradient and spectral parameters were set according to Reingold et al. (2022) [20]. Identification was accomplished by comparison of experimental monoisotopic masses with data present in literature and with an in-house fungal database of secondary metabolites.

GC–MS analysis

An aliquot of the EtOAc extract undergone a derivatization procedure prior to GC–MS analysis. Briefly, the fraction was resuspended in EtOAc at 100 ppm as final concentration and the solution was derivatized with N,O-bis(trimethylsilyl)-trifluoroacetamide (BSTFA) (Fluka, Buchs, Switzerland) for 30 min in an ultrasonic bath (Sonorex, Bandelin electronic GmbH & Co. K, Berlin, Germany). Derivatized sample was analyzed by an Agilent 5977B MSD mass spectrometer coupled to an Agilent 8890 GC (Agilent Technologies). Chromatographic and spectrometric parameters were set using the MassHunter Workstation software version 10.1.49 (Agilent Technologies), according to the method described by Vinale et al. (2020) [21]. Identification of metabolites was achieved by comparison of deconvoluted mass spectra with known compounds, whose spectra are collected in NIST (National Institute of Standards and Technology) 20 library [22]. Identification was also supported by calculation of Kovats retention index (RI) for each analyte, using the standard *n*-alkane mixture in the range C7-C40 (Sigma-Aldrich, Saint Louis, MO, USA).

Single crystal X-ray analysis

Single crystals of chromone complex were prepared at room temperature by slow evaporation of ethyl acetate. Chromone crystals appeared as transparent elongated plates with typical dimensions of 0.1 × 0.03 × 0.03 mm. Data were collected with synchrotron radiation (wavelength, 0.7000 Å) from XRD1 beamline at the Elettra Synchrotron Light Source, Trieste Italy. By using a small loop of fine rayon fiber, the selected crystal for data diffraction was dipped in cryoprotectant Paratone oil and flash frozen in a stream of nitrogen at 100 K. For the best diffracting crystal, a total of 360-degree crystal rotation data were collected from 720 images using an oscillation range of 0.5. Data were processed using XDS and POINTLESS 1.11.21 with a data collection statistic reported in Table 1 [23]. Crystal gave a monoclinic unit cell with axes a = 7.42 Å, b = 7.90 Å, c = 9.69 Å, α = 72.10°, β = 72.23° γ = 78.84°, V = 511 Å^3, and space group P -1. Structure solution was found by direct methods using Sir200 [24], which revealed the presence of one molecule in the ASU and most of the expected metabolite atom connectivity. Structure was anisotropically refined using full matrix least-squares methods on F^2 against all independent measured reflections using SHELXL [25] run under WinGX [26] suite for the refinement of small molecules. Peaks in difference electron density map were observed corresponding to all hydrogen atoms of the metabolite, which were introduced and refined in agreement with a riding model as implemented in SHELXL. Figures were generated using Mercury CSD 3.6 [27]. Chromone crystallographic data have been deposited with

Table 1 Crystal data and structure refinement details for methoxychromone derivative (**1**)

	Methoxychromone derivative (1)
CCDC number	2142932
Metabolite formula	$C_{12}H_{12}O_4$
Temperature (K)	100
Wavelength (Å)	0.7000
Crystal system	Triclinic
Space group	*P -1*
a (Å)	7.4160(15)
b (Å)	7.9020(16)
c (Å)	9.6910(19)
α (°)	72.10(3)
β (°)	72.23(3)
γ (°)	78.84(3)
R-merge (last shell: 0.75–0.71 Å)	0.055 (0.224)
CC(1/2)	1.000 (0.982)
I/s(I)	10.11 (4.08)
Completeness (%)	97.5 (96.5)
Estimated mosaicity (°)	0.236
Volume	511.51 Å^3
Z	2
Calculated density	1.430 g cm^{-3}
q range for data collection (°)	2.684–29.756
All data / restraints / parameters	2999/0/149
R1 indices (I > 2 s(I), 1873)	0.0586
wR2	0.207, all data
F(000)	232
Largest diff. peak and hole	0.404 and − 0.382 e-/Å^3
Goodness-of-fit on F^2	0.82

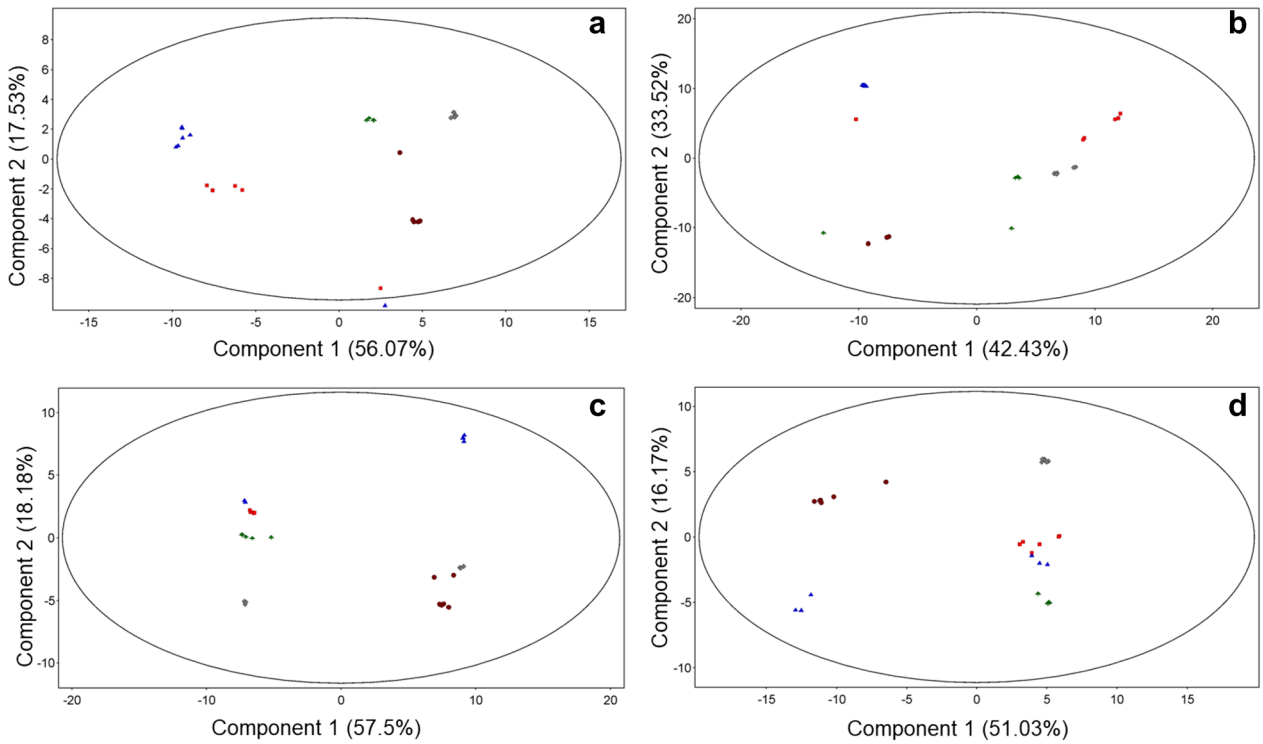

Fig. 1 Principal component analysis (PCA) score plots of the LC–MS data from M10 culture filtrates. Each medium is depicted with a different color and shape: PDB is brown circle; 1/10 PDB is gray rhombus; MM is red square; MM + Fe is blue triangle, YPD is green arrow. **a** dark + shaking condition: PC1 accounts for 56.07% and PC2 17.53% of total variance; **b** light + shaking condition: PC1 42.43% and PC2 33.52%; **c** dark + static condition: PC1 57.5% and PC2 18.18%; **d** light + static condition: PC1 51.03% and PC2 16.17%

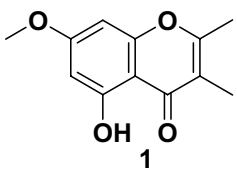

1

Fig. 2 Structure of 5-hydroxy-2,3-dimethyl-7-methoxychromone (**1**)

the Cambridge Crystallographic Data Centre and can be obtained via www.ccdc.cam.ac.uk/data_request/cif with the accession code 2142932 [28]. A selection of crystal data and structure refinement details for methoxychromone derivative are reported in Table 1.

Antifungal assay

Purified methoxychromone derivative was tested against soil-borne plant pathogen *R. solani* using the method described by Vinale et al. (2016) with some modifications [29]. Starting from actively growing mycelium, 5 mm Ø plugs were placed at the center of Petri dished containing PDA. Volumes of 10 µL were applied on each plug at six different concentrations, ranging from 0.01 to 200 µg plug^{-1}. Water and ethyl acetate-treated plugs were used as controls. Petri plates were left in a laminar flow cabinet until the solvent was evaporated and then incubated for four days at room temperature. Radial growth was measured daily as colony diameter (mm) and used to calculate the inhibition percentage.

Plant growth promotion assay

To test the plant growth promotion activity, tomato seeds (*Lycopersicum esculentum* cv. San Marzano 823) were treated (coating) with different amounts of **1** (from 200 µg to 1 ng per seed). The method described by Vinale et al. (2009) was used to determine the effect on seed germination and plant growth [30].

Cytotoxicity assay

The human colon adenocarcinoma cell lines HCT116 (ATCC from LGC Standards, Milan, Italy) were cultured in Dulbecco's Modified Eagle Medium (DMEM, Sigma-Aldrich, Milan, Italy) supplemented with 10% and heat-inactivated Fetal Bovine Serum (FBS, Sigma-Aldrich,

Table 2 Metabolites differentially accumulated in M10 culture filtrates cultivated in different media (MM, MM + Fe, YPD, PDB, 1/10 PDB) and under different conditions (dark + shaking, light + shaking, dark + static, light + static)

Compound	Regulation			
	PDB vs MM	PDB vs MM + Fe	PDB vs YPD	PDB vs 1/10 PDB
Dark + shaking				
T39butenolide	↑	↑	↑	↓
Harzianolide	↓	↓	↑	↓
Light + shaking				
Dehydro harzianolide	↓	↓	↓	↓
5-hydroxy-2,3-dimethyl-7-methoxychromone	↑	↑	↑	↑
Harzianolide	↓	↓	↓	↓
Harzianic acid	↓	↑	↓	↓
Ferricrocin	↓	↓	↓	↓
Dark + static				
Dehydro harzianolide	↑	↑	↑	↑
Harzianolide	↑	↑	↑	↑
Isoharzianic acid	↑	↑	↑	↓
Harzianic acid	↑	↑	↑	↓
Light + static				
Dehydro harzianolide	↑	↓	↑	↓
T39butenolide	↓	↓	↓	↓
Dimethyl-harzianic acid	↑	↑	↑	↓
Isoharzianic acid	↑	↑	↑	↓
Harzianic acid	↑	↑	↑	↓
Homoharzianic acid	↓	↓	↓	↓
Coprogen B	↓	↓	↓	↓

↓ = down-regulated, PDB *vs* other media; ↑ is up-regulated, PDB *vs* other media

Milan, Italy) and maintained at 37 °C in a humidified incubator with 5% CO_2. Cell viability was evaluated by measuring the mitochondrial reductase activity (MTT assay). Briefly, HCT116 cells were seeded in a 96-wells plate (1×10^4 cells per well) and then treated for 48 h with compound **1** (0.1–10 µg/mL). After this period, the treatment medium was replaced with fresh medium containing MTT (250 µg/mL, for 1 h at 37 °C). After solubilization in DMSO, the mitochondrial reduction of MTT to formazan was quantitated at 490 nm using Multiskan GO microplate reader (Thermo Fisher Scientific, MA, USA).

Statistical analysis

Statistical analysis was performed on culture filtrates of *T. harzianum* M10 cultivated under different conditions (OSMAC strategy) to evaluate statistical differences of the production of secondary metabolites. Multivariate and univariate analyses were implemented following the method described by Comite et al. (2021) [31].

Statistical differences among treatments applied on *R. solani* plugs and control group were evaluated by performing one-way ANOVA followed by Dunnett's multiple comparisons test ($p < 0.001$) on GraphPad Prism software version 9.4.1 (GraphPad Software, San Diego, California USA). The same approach was used to estimate significant reduction of human colon adenocarcinoma cells viability of treated samples against control group.

Results and discussion

T. harzianum M10 was cultured in different liquid media (potato dextrose broth—PDB −, 1/10 diluted PDB, yeast peptone glucose−−YPD, minimal medium−−MM, and MM + 1 mM of $FeCl_3$) and under different conditions (light or dark, static or shaking—140 rpm—for 15 days at 25 °C) to evaluate the modulation of metabolic profiles.

Raw data, obtained after LC–MS analysis of culture filtrates, were subjected to statistical analysis (multivariate, principal component analysis; univariate, one-way ANOVA $p < 0.05$ and fold change (FC) > 2.0). The score plots for each couple of conditions (dark + shaking, light + shaking, dark + static, light + static) are reported in Fig. 1.

A clear separation along components is evident, particularly for principal component 1. Figure 1a shows the formation of two subgroups composed of MM and MM + Fe samples on the left side of the plot, and YPD, PDB, and 1/10 PDB that spread along PC2 on the right side of the plot. Similar trends are showed in Fig. 1b–d, with a separation in two subgroups that are differently composed. MM is grouped with richer media (YPD and 1/10 PDB), and PDB samples cluster away from both rich and poor media (Fig. 1b, c). Under light + static condition (Fig. 1d), poor media cluster together and are closer in the component space to YPD group, while 1/10 PDB separates along PC2. PDB group is separated along both PC1 and PC2. For each multivariate analysis it is possible to notice an unsupervised separation, the presence of subgroupings within replicates, and one outlier falling outside the 95% confidence ellipse in Fig. 1a. Unusual behaviors are due to biological variability of the samples.

Table 3 Compounds identified from *T. harzianum* M10 crude extract by GC and LC–MS analysis

Compound	Rt (min)	RI
GC–MS		
2,3-Butanediol, 2TMS derivative	5.469	1054.3
2-Hydroxy-3-methylbutyric acid, 2TMS derivative	7.158	1175.1
2-Hydroxyisocaproic acid, 2TMS derivative	8.133	1244.0
Hexanoic acid, 2TMS derivative	8.186	1247.7
Glycerol, 3TMS derivative	8.699	1283.7
Nicotinic acid, TMS derivative	8.874	1296.1
1,2,3-Butanetriol, 3TMS derivative	9.000	1305.3
Pentanedioic acid, 2TMS derivative	10.349	1407.9
Furandimethanol, 2TMS derivative	10.532	1422.8
3-Hydroxy-2,3-dihydromaltol, 2TMS derivative	10.997	1461.1
DL-Pyroglutamic acid, 2TMS derivative	11.775	1535.8
5-Hydroxy-2-(hydroxymethyl)pyridine, 2TMS derivative	11.873	1545.6
3-Phenyllactic acid, 2TMS derivative	12.332	1598.1
4-Hydroxybenzoic acid, 2TMS derivative	12.588	1636.1
Cyclo(glycylprolyl), TMS derivative	13.249	1743.2
Protocatechuic acid, 3TMS derivative	13.713	1833.5
Homoprotocatechuic acid, 3TMS derivative)	13.772	1846.4
Stearic acid, TMS derivative	15.300	2238.8
Uridine, 4TMS derivative	16.313	2476.5
Compound	**Monoisotopic mass (Da)**	**Molecular formula**
LC–MS		
2-Aminophenylacetic acid	151.0636	$C_8H_9NO_2$
Nicotinic acid	123.0325	$C_6H_5NO_2$
Benzeneacetaldehyde	120.0579	C_8H_8O
Indoleacetic acid	205.0861	$C_{12}H_{13}O_3$
7-Hydroxy-3-(2,3-dihydroxybutyl)-1(3H)-isobenzofuranone	238.0828	$C_{12}H_{14}O_5$
Tryptophol	161.0843	$C_{10}H_{11}NO$
Isoharzianic acid	365.1844	$C_{19}H_{27}NO_6$
5-hydroxy-2,3-dimethyl-7-methoxychromone	220.0758	$C_{12}H_{12}O_4$
Harzianic acid	365.1852	$C_{19}H_{27}NO_6$
Homoharzianic acid	379.2003	$C_{20}H_{29}NO_6$

Metabolic profiles resulted to be strongly influenced by the medium and environmental conditions.

Due to the promising results obtained from PCAs, univariate analysis was performed to identify metabolites, whose abundance and production were influenced by the cultivating condition. Among the statistically different compounds detected (69, 175, 100, 104 for dark + shaking, light + shaking, dark + static and light + static, respectively), it was possible to identify siderophores, such as ferricrocin and coprogen B, harzianic acid (HA) and its derivatives, butenolides and a never isolated from M10 metabolite, 5-hydroxy-2,3-dimethyl-7-methoxychromone (**1,** Fig. 2). In Table 2 the regulation of metabolites (up- or down-regulated), analyzed in M10 culture filtrate in different substrates and conditions, is reported.

Interestingly, the chromone derivative is up-regulated when M10 strain has been cultivated in PDB under shaking and white light condition. Furthermore, HA and isoHA production increased in diluted PDB in all conditions except for dark + shaking. Concerning HA derivatives, it was possible to detect homoHA and dimethylHA only in static cultivations, with remarkable modulation when M10 is grown under white light (Table 2).

T. harzianum M10 was then cultivated in higher volumes of medium under inducing conditions (PDB, shaking and white light, at 25 °C) to purify and

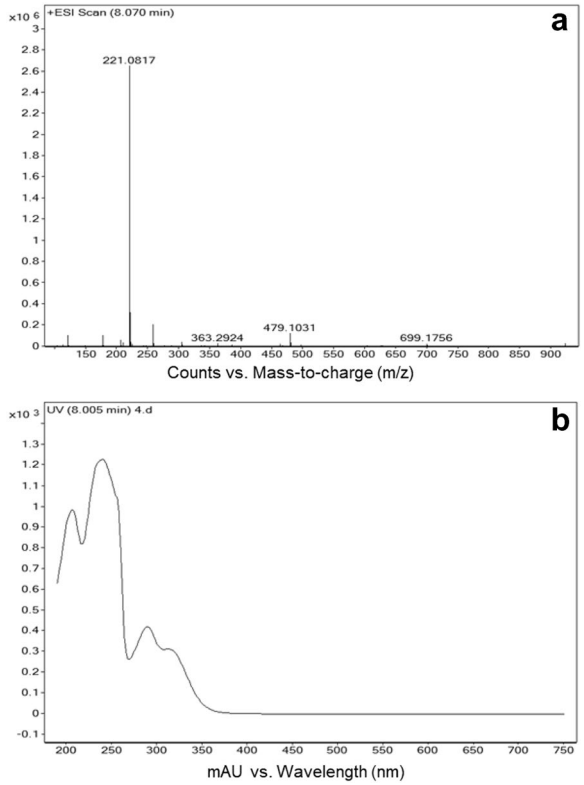

Fig. 3 Mass spectrum of 1 (**a**); UV–Vis spectrum of 1 (**b**)

characterize the unknown compound. The culture filtrate was exhaustively extracted with EtOAc, and the crude extract suspended in DCM and washed with diluted NaOH to remove HA and its derivatives (including stereoisomers). EtOAc extracts were analyzed by GC–MS and LC–MS: the known compounds reported in Table 3 were readily identified by spectroscopic and chromatographic data comparison with libraries, and by comparison with authentic standards.

The DCM residue was separated by silica gel column chromatography to give sixteen fractions. Fractions from 2 to 6 (21.3 mg) contained compound **1** as pure crystals (Fig. 2).

5-hydroxy-2,3-dimethyl-7-methoxychromone (**1**) (2.1 mg L^{-1}) was a transparent crystal with a molecular ion $[M+H]^+$ at 221.0817, $[M+K]^+$ at 259.0286, $[2\ M+K]^+$ at 479.1031, $[3\ M+K]^+$ at 699.1756, and λ max at 205, 240, 289, and 316 nm (Fig. 3a and b). UV, IR, and NMR (Additional file 1: Fig. S1 and S2, Table S1) spectroscopic data are consistent with data from literature [32].

The X-ray structure of the chromone is shown in Fig. 4. The probe crystallizes in centrosymmetric space group *P*-1 with one molecule in the asymmetric unit. Crystal packing of chromone shows antiparallel arrangement of the metabolite and exhibits π–π stacking interactions of the molecule core structure along the a-axis, in agreement with the inversion center of P-1 space group (Fig. 4). The structure is stabilized by the intramolecular hydrogen bond of 2.582 Å between the -OH group and oxygen atom group of the ketone moiety.

The compound 5-hydroxy-2,3-dimethyl-7-methoxychromone, purified for first time from *T. harzianum* strain M10, both in the culture filtrate (exometabolites) and on the mycelia (endometabolites), was tested at different concentrations for antifungal activity against the phytopathogenic agent *R. solani*. Antifungal activity was increased with the increasing concentration of compound **1**. The maximum inhibition percentage

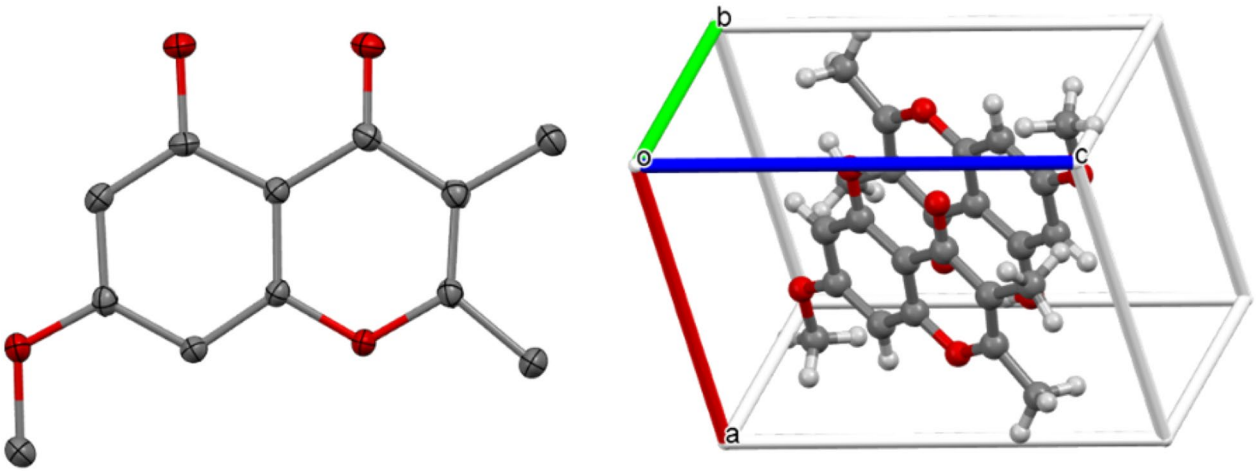

Fig. 4 Thermal ellipsoids representation of chromone drawn at 50% probability (left side) and crystal packing arrangement of chromone (right side). Atoms are color coded as follows: carbon (gray), oxygen (red), nitrogen (blue) in balls-and-sticks representation. Crystal packing arrangement shows pi-pi interactions along the *b*-axis

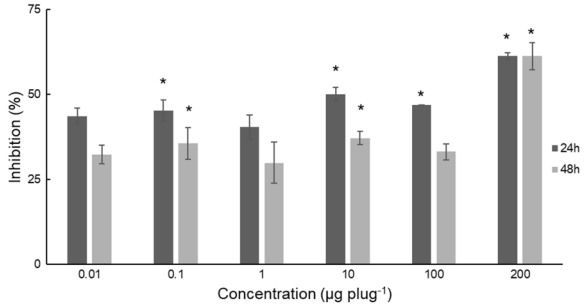

Fig. 5 Inhibition of *Rhizoctonia solani* radial growth after treatment with 5-hydroxy-2,3-dimethyl-7-methoxychromone (1) at different concentrations. Bars represent standard deviation. *$p < 0.001$ according to one-way ANOVA statistical analysis against control group

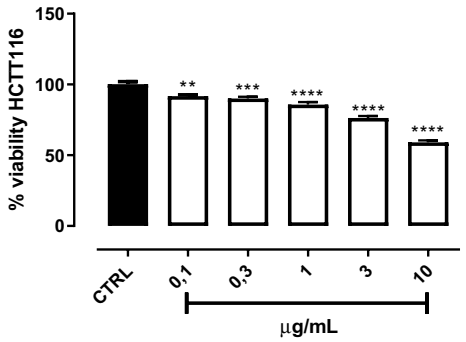

Fig. 6 Cell viability assay in HCT116 cells alone (CTRL) or in the presence of 5-hydroxy-2,3-dimethyl-7-methoxychromone (**1**) at different concentrations (0.1–10 µg/mL, 48 h) ($n = 3$). Results are expressed as mean ± SEM

was 61% after 24 h of incubation at a concentration of 200 µg plug^{-1}, whereas the lowest concentration that resulted in a significant inhibition (45%) against control was 100 ng plug $^{-1}$ after 24 h of incubation (Fig. 5).

In our experiments, tomato seedlings assays showed that (**1**) do not promote plant growth even at low concentration. No significant phytotoxic effects have been registered at all the concentration used (data not shown).

The cytotoxic effect of 5-hydroxy-2,3-dimethyl-7-methoxychromone (**1**) was detected against the colorectal human cancer cell line HCT116. As shown in Fig. 6, treatment with compound **1** significantly reduced the viability of HCT116 cells in a concentration-dependent manner after 48 h of incubation (40% reduction of viability at 10 µg mL^{-1}; 25% at 3 µg mL^{-1}; 15% at 1 µg mL^{-1}, and 10% at 0.3 and 0.1 µg mL^{-1}).

5-hydroxy-2,3-dimethyl-7-methoxychromone has been isolated from *T. citrinoviride* but no bioactivity has been reported [33]. Interestingly, **1**, purified form a marine *Trichoderma* sp. (strain TA26-28), showed a significant antibiotic activity against several pathogenic bacteria (six Gram-positive *Staphylococcus aureus*, *S. albus*, *Bacillus cereus*, *B. subtilis*, *Micrococcus tetragenus*, *Kocuria rhizophila*, and four Gram-negative *Escherichia coli*, *Vibrio parahaemolyticus*, *V. anguillarum*, and *Pseudomonas putida*) with minimum inhibitory concentration ranging from 0.78 to 6.25 µM [34]. The chromone derivative, purified from the endophytic *T. harzianum* strain Fes1712, demonstrated low antimicrobial activity against *C. albicans, B. subtilis, E. coli, P. aeruginosa,* and *S. aureus* with MIC values > 256 µg mL^{-1} [35]. Recently, Siebatcheu et al. (2022) reported that **1**, extracted from liquid cultures of *T. erinaceum*, inhibited the mycelial growth of *Pythium ultimum* (200 µg mL^{-1} = 46.05% of inhibition; 100 ng mL^{-1} = 17.11% of inhibition) [36].

Zhang et al. (2021) reported the antifungal activity and MIC value determined by microdilution assays of the similar pure compound, 5-hydroxy-3-hydroxymethyl-2-methyl-7methoxychromone isolated from a strain of *T. harzianum* [37]. This compound showed significant activity (MIC of 256 µg mL^{-1}) against the causal agent of anthracnose on several fruits, *Colletotrichum gloeosporioides* [38].

Compound **1** has been isolated from other microbial strains, such as the entomopathogenic fungus *Aschersonia confluens* BCC53152 (antibacterial activity tested against *B. cereus*, *E. coli*, *P. aeruginosa, Klebsiella pneumoniae*, *Acinetobacter baumannii,* and *Enterococcus faecium* with MIC values > 50 µg mL^{-1}; cytotoxicity activity against Vero cells with IC50 value of 194.90 µM) [39], the mycobiont cultures of the lichen *Graphis scripta* [32], and *Talaromyces minioluteus*, from the deep-sea cold seep mussel *Gigantidas platifrons*. In this last work the authors named the compound as 5-hydroxy-7-methoxy-2,3-dimethylchromone [40].

Chromones are isolated in plants and microbes and are heterocyclic compounds having a benzoannelated γ-pyrone ring representing the core of a fragment of various flavonoids. Numerous molecules belonging to this class of natural products have significant biological activities and are reported to be used in traditional medicines as antiallergic, anti-inflammatory, antidiabetic, antitumor, anti-asthma/bronchodilator, and antimicrobial (also including development of chromone-based drugs) [41]. Anticancer activity has been also related to various chromones for several molecular targets, such as protein kinases, protein tyrosine phosphatases, thymidine

phosphorylase, topoisomerase, and drug transporters [42].

Conclusion

Microorganisms play a key role as main source of secondary metabolites for pharmaceutical and agricultural purposes. Nevertheless, the number of new metabolites is decreasing due to the purification of known compounds. OSMAC strategy can overcome laboratory limitations and allow the discovery of novel metabolites, whose biosynthetic pathways are activated or up-regulated by different growing conditions. The application of sets of conditions and different liquid media modulated M10 metabolic profiles: harzianic acid, its derivatives, and other known compounds were up or down-regulated depending on the experimental setup. The combination of shaking, light and PDB elicited the production of a never isolated from M10 compound. The methoxychromone derivative was obtained as pure crystals, characterized by X-ray diffraction and mass spectrometry, and tested for antimicrobial and antitumor activities.

Abbreviations

OSMAC	One Strain MAny Compounds
PDB	Potato dextrose broth
DMSO	Dimethyl sulfoxide
TLC	Thin-layer chromatography
PDA	Potato dextrose agar
YPD	Yeast peptone glucose
MM	Minimal medium
DCM	Dichloromethane
EtOAc	Ethyl acetate
DAD	Diode array detector
BSTFA	N,O-bis(trimethylsilyl)trifluoroacetamide
FC	Fold change
LC–MS	Liquid chromatography–mass spectrometry
GC–MS	Gas chromatography–mass spectrometry
PCA	Principal component analysis
HA	Harzianic acid
MIC	Minimal inhibitory concentration
DMEM	Dulbecco's Modified Eagle Medium
FBS	Fetal Bovine Serum
MTT	3-(4,5-Dimethylthiazol-2-yl)-2,5-diphenyltetrazolium bromide

Supplementary Information

The online version contains supplementary material available at https://doi.org/10.1186/s40538-023-00383-x.

Additional file 1: Figure S1. IR spectrum of 5-hydroxy-2,3-dimethyl-7-methoxychromone. **Figure S2.** ^{1}H-NMR spectrum of 5-hydroxy-2,3-dimethyl-7-methoxychromone. **Table S1**. ^{1}H-NMR Spectral Data of 5-hydroxy-2,3-dimethyl-7-methoxychromone, measured in $CDCl_3$.

Acknowledgements

The authors are grateful to Prof. Anna Andolfi and Dr. Maria Michela Salvatore for performing NMR and IR experiments and providing the interpretation.

Author contributions

FV and SLW contributed to conceptualization; AS and FV contributed to methodology; AS, PDC, GI, and LDC performed investigation; AS, GI, PDC, and LDC were involved in data curation; AS and FV prepared original draft; all the authors were involved in review and editing:. All the authors have read and approved to the published version of the manuscript.

Funding

This study was carried out within the Agritech National Research Center and received funding from Bio Inspired Plant Protection project, PRIN 2020 2020T58TA3, and the European Union Next-Generation EU (PIANO NAZIONALE DI RIPRESA E RESILIENZA (PNRR)—MISSIONE 4 COMPONENTE 2, INVESTIMENTO 1.4—D.D. 1032 17/06/2022, CN00000022). This manuscript reflects only the authors' views and opinions neither the European Union nor the European Commission can be considered responsible for them.

Availability of data and materials

The data sets used and/or analyzed during the current study are available to readers as in the manuscript and from the corresponding author upon reasonable request.

Declarations

Ethics approval and consent to participate

Not applicable.

Consent for publication

Not applicable.

Competing interests

The authors declare that they have no competing interests.

Author details

[1]Department of Agricultural Sciences, University of Naples Federico II, 80055 Portici, Italy. [2]Institute for Sustainable Plant Protection, National Research Council, 80055 Portici, Italy. [3]Department of Pharmacy, University of Naples Federico II, 80100 Naples, Italy. [4]Department of Veterinary Medicine and Animal Production, University of Naples Federico II, 80137 Naples, Italy. [5]BAT Center-Interuniversity Center for Studies on Bioinspired Agro-Environmental Technology, University of Naples Federico II, 80055 Portici, Italy.

Received: 7 December 2022 Accepted: 16 January 2023
Published online: 28 March 2023

References

1. Carillo P, Woo SL, Comite E, El-Nakhel C, Rouphael Y, Fusco GM, et al. Application of *Trichoderma harzianum*, 6-pentyl-α-pyrone and plant biopolymer formulations modulate plant metabolism and fruit quality of plum tomatoes. Plants. 2020;11:771. https://doi.org/10.3390/plants9060771.
2. Vinale F, Sivasithamparam K, Ghisalberti EL, Marra R, Woo SL, Lorito M. *Trichoderma*–plant–pathogen interactions. Soil Biol Biochem. 2008;2008(40):1–10. https://doi.org/10.1016/j.soilbio.2007.07.002.
3. Woo SL, Hermosa R, Lorito M, Monte M. *Trichoderma*: a multipurpose, plant-beneficial microorganism for eco-sustainable agriculture. Nat Rev Microbiol. 2022. https://doi.org/10.1038/s41579-022-00819-5.
4. Lorito M, Woo SL, Harman GE, Monte E. Translational research on *Trichoderma*: from 'omics to the field. Annu Rev Phytopathol. 2010;48:395–417. https://doi.org/10.1146/annurev-phyto-073009-114314.
5. Mazzei P, Vinale F, Woo SL, Pascale A, Lorito M, Piccolo A. Metabolomics by proton high-resolution magic-angle-spinning nuclear magnetic resonance of tomato plants treated with two secondary metabolites isolated from *Trichoderma*. J Agric Food Chem. 2016;64:3538–45. https://doi.org/10.1021/acs.jafc.6b00801.
6. Mayo-Prieto S, Marra R, Vinale F, Rodríguez-González Á, Woo SL, Lorito M, et al. Effect of *Trichoderma velutinum* and *Rhizoctonia solani* on

the metabolome of bean plants (*Phaseolus vulgaris* L.). Int J Mol Sci. 2019;20:549. https://doi.org/10.3390/ijms20030549.
7. Marra R, Coppola M, Pironti A, Grasso F, Lombardi N, d'Errico G, et al. The application of *Trichoderma* strains or metabolites alters the olive leaf metabolome and the expression of defense-related genes. J Fungi. 2020;6:369. https://doi.org/10.3390/jof6040369.
8. Staropoli A, Vassetti A, Salvatore MM, Andolfi A, Prigigallo MI, Bubici G, et al. Improvement of nutraceutical value of parsley leaves (*Petroselinum crispum)* upon field applications of beneficial microorganisms. Horticulturae. 2021;7:281. https://doi.org/10.3390/horticulturae7090281.
9. Sivasithamparam K, Ghisalberti EL. Secondary metabolism in *Trichoderma* and *Gliocladium*. In: Harman GE, Kubicek CP, editors. *Trichoderma* and *Gliocladium*, vol. 1. London: Taylor and Francis Ltd.; 1998. p. 139–91.
10. Zeilinger S, Gruber S, Bansal R, Mukherjee PK. Secondary metabolism in *Trichoderma*–chemistry meets genomics. Fungal Biol Rev. 2016;30:74–90. https://doi.org/10.1016/j.fbr.2016.05.001.
11. Vinale F, Sivasithamparam K. Beneficial effects of *Trichoderma* secondary metabolites on crops. Phytother Res. 2020;34:2835–42. https://doi.org/10.1002/ptr.6728.
12. Vinale F, Sivasithamparam K, Ghisalberti EL, Ruocco M, Wood S, Lorito M. *Trichoderma* secondary metabolites that affect plant metabolism. Nat Prod Commun. 2012;7:1545–50.
13. Baral B, Akhgari A, Metsä-Ketelä M. Activation of microbial secondary metabolic pathways: avenues and challenges. Synth Syst Biotechnol. 2018;3:163–78. https://doi.org/10.1016/j.synbio.2018.09.001.
14. Bode HB, Bethe B, Höfs R, Zeeck A. Big effects from small changes: possible ways to explore nature's chemical diversity. ChemBioChem. 2002;3:619–27. https://doi.org/10.1002/1439-7633(20020703)3:7%3c619::AID-CBIC619%3e3.0.CO;2-9.
15. Scherlach K, Hertweck C. Triggering cryptic natural product biosynthesis in microorganisms. Org Biomol Chem. 2009;7:1753. https://doi.org/10.1039/b821578b.
16. Sanchez JF, Somoza AD, Keller NP, Wang CC. Advances in *Aspergillus* secondary metabolite research in the post-genomic era. Nat Prod Rep. 2012;29:351–71. https://doi.org/10.1039/c2np00084a.
17. Pinedo-Rivilla C, Aleu J, Durán-Patrón R. Cryptic Metabolites from marine-derived microorganisms using OSMAC and epigenetic approaches. Mar Drugs. 2022;20:84. https://doi.org/10.3390/md20020084.
18. Vinale F, Nicoletti R, Borrelli F, Mangoni A, Parisi OA, Marra R, et al. Co-culture of plant beneficial microbes as source of bioactive metabolites. Sci Rep. 2017;7:14330. https://doi.org/10.1038/s41598-017-14569-5.
19. De Filippis A, Nocera FP, Tafuri S, Ciani F, Staropoli A, Comite E, et al. Antimicrobial activity of harzianic acid against *Staphylococcus pseudintermedius*. Nat Prod Res. 2021;35:5440–5. https://doi.org/10.1080/14786419.2020.1779714.
20. Reingold V, Staropoli A, Faigenboim A, Maymone M, Matveev S, Kepanan R, et al. The SWC4 subunit of the SWR1 chromatin remodeling complex is involved in varying virulence of *Metarhizium brunneum* isolates offering role of epigenetic regulation of pathogenicity. Virulence. 2022;13:1252–69. https://doi.org/10.1080/21505594.2022.2101210.
21. Vinale F, Salvatore MM, Nicoletti R, Staropoli A, Manganiello G, Venneri T, et al. Identification of the main metabolites of a marine-derived strain of *Penicillium brevicompactum* using LC and GC MS techniques. Metabolites. 2020;10:55. https://doi.org/10.3390/metabo10020055.
22. NIST 20. Available online: https://www.nist.gov/srd/nist-standard-reference-database-1a (accessed on October 18th 2022).
23. Evans PR. An introduction to data reduction: space-group determination, scaling and intensity statistics. Acta Crystallogr D Biol Crystallogr. 2011;67:282–92. https://doi.org/10.1107/S090744491003982X.
24. Burla MC, Carrozzini B, Cascarano GL, Giacovazzo C, Polidori G. Solving proteins at non-atomic resolution by direct methods: update. J Appl Crystallogr. 2017;50:1048–55. https://doi.org/10.1107/S1600576717007300.
25. Sheldrick GM. SHELXT—integrated space-group and crystal-structure determination. Acta Crystallogr A Found Adv. 2015;71:3–8. https://doi.org/10.1107/S2053273314026370.
26. Farrugia LJ. WinGX and ORTEP for Windows: an update. J Appl Crystallogr. 2012;45:849–54. https://doi.org/10.1107/S0021889812029111.
27. MacRae CF, Sovago I, Cottrell SJ, Galek PTA, McCabe P, Pidcock E, et al. Mercury 4.0: from visualization to analysis, design and prediction. J Appl Crystallogr. 2020;53:226–35. https://doi.org/10.1107/S1600576719014092.
28. Cambridge Crystallographic Data Centre, available online at: www.ccdc.cam.ac.uk/data_request/cif.
29. Vinale F, Strakowska J, Mazzei P, Piccolo A, Marra R, Lombardi N, et al. Cremenolide, a new antifungal, 10-member lactone from *Trichoderma cremeum* with plant growth promotion activity. Nat Prod Res. 2016;30:2575–81. https://doi.org/10.1080/14786419.2015.1131985.
30. Vinale F, Flematti G, Sivasithamparam K, Lorito M, Marra R, Skelton BW, Ghisalberti EL. Harzianic acid, an antifungal and plant growth promoting metabolite from *Trichoderma harzianum*. J Nat Prod. 2009;72:2032–5. https://doi.org/10.1021/np900548p.
31. Comite E, El-Nakhel C, Rouphael Y, Ventorino V, Pepe O, Borzacchiello A, et al. Bioformulations with beneficial microbial consortia, a bioactive compound and plant biopolymers modulate sweet basil productivity, photosynthetic activity and metabolites. Pathogens. 2021;10:87. https://doi.org/10.3390/pathogens10070870.
32. Tanahashi T, Takenaka Y, Nagakura N, Hamada N. 2,3-Dialkylchromones from mycobiont cultures of the lichen *Graphis Scripta*. Heterocycles. 2000;53:1589–93.
33. Liang XR, Miao FP, Song YP, Guo ZY, Ji NY. Trichocitrin, a new fusicoccane diterpene from the marine brown alga-endophytic fungus *Trichoderma citrinoviride* cf-27. Nat Prod Res. 2016;30:1605–10. https://doi.org/10.1080/14786419.2015.1126264.
34. Qin XY, Yang KL, Wang CY, Shao CL. Secondary metabolites of the zoanthid-derived fungus *Trichoderma* sp. TA26–28 collected from the south China sea. Chem Nat Compd. 2014;50:961–4. https://doi.org/10.1007/s10600-014-1134-2.
35. Ding Z, Tao T, Wang L, Zhao Y, Huang H, Zhang D, et al. Bioprospecting of novel and bioactive metabolites from endophytic fungi isolated from rubber tree *Ficus elastica* leaves. J Microbiol Biotechnol. 2019;29:731–8. https://doi.org/10.4014/jmb.1901.01015.
36. Siebatcheu EC, Wetadieu D, Youassi O, Bedine Boat MA, Bedan KG, Tchameni NS, et al. Secondary metabolites from an endophytic fungus Trichoderma erinaceum with antimicrobial activity towards Pythium ultimum. Nat Prod Res. 2022;18:1–6. https://doi.org/10.1080/14786419.2022.2075360.
37. Zhang JL, Tang WL, Huang QR, Li YZ, Wei ML, Jiang LL, et al. *Trichoderma*: a treasure house of structurally diverse secondary metabolites with medicinal importance. Front Microbiol. 2021;12:723828. https://doi.org/10.3389/fmicb.2021.723828.
38. Jeerapong C, Phupong W, Bangrak P, Intana W, Tuchinda P. Trichoharzianol, a new antifungal from *Trichoderma harzianum* F031. J Agric Food Chem. 2015;63(14):3704–8. https://doi.org/10.1021/acs.jafc.5b01258.
39. Sadorn K, Saepua S, Punyain W, Saortep W, Choowong W, Rachtawee P, et al. Chromanones and aryl glucoside analogs from the entomopathogenic fungus Aschersonia confluens BCC53152. Fitoterapia. 2020;144:104606. https://doi.org/10.1016/j.fitote.2020.104606.
40. Song Q, Yang SQ, Li XM, Hu XY, Li X, Wang BG. Aromatic polyketides from the deep-sea cold-seep mussel associated endozoic fungus *Talaromyces minioluteus* CS-138. Mar Drugs. 2022;20:529. https://doi.org/10.3390/md20080529.
41. Keri RS, Budagumpi S, Pai RK, Balakrishna RG. Chromones as a privileged scaffold in drug discovery: a review. Eur J Med Chem. 2014;78:340–74. https://doi.org/10.1016/j.ejmech.2014.03.047.
42. Patil VM, Masand N, Verma S, Masand V. Chromones: privileged scaffold in anticancer drug discovery. Chem Biol Drug Des. 2021;98:943–53. https://doi.org/10.1111/cbdd.13951.

Publisher's Note